Chapter 1

Introduction, Literature Survey and Objective

1.1. Organic pollutants: A severe environmental threat

Population growth always accompanies greater demand for natural resources like water and the establishment of industries to fulfill its needs (Cosgrove & Loucks, 2015). Many industries such as chemical, petrochemical, pharmaceutical, mining, semiconductor, and microelectronics have been set up worldwide to fulfill higher demand for goods (Holling & Meffet, 1996). In addition, the world's increasing population is also escalating the water requirement for drinking and household purposes. Each of these industries requires large quantities of water for processing. Most of the water discharged from these industries is contaminated with toxic organic pollutants (Pimentel, et. al, 2004) or compounds. Often, they are by-products of industrial operations or industrial chemicals. Organic contaminants can be present in the air, the soil, and the water (Adithya et al., 2021; Gianfreda et al., 2005; Subashchandrabose et al., 2013) (Fig. 1.1).

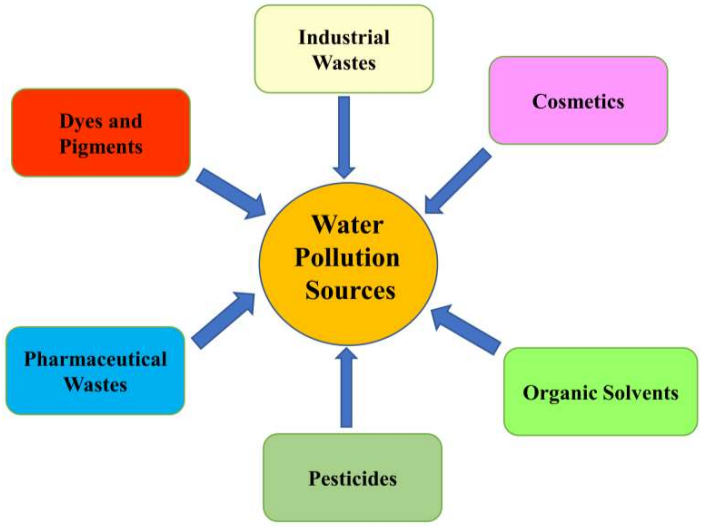

Fig. 1.1: Common sources of organic pollutants in water pollution

Organic pollutants are particularly hazardous because they are difficult to degrade and can build up in human and animal fat. These substances can potentially harm the immune system, and cause cancer and reproductive problems, even in small doses (Guo et al., 2019). They are also a serious threat to biodiversity, birds, and

animals. It is observed that they cause behavioural abnormalities and congenital disabilities in fish, birds, and mammals (El-Shahawi et al., 2010; Jones & De Voogt, et. al, 1999.) (Fig. 1.2).

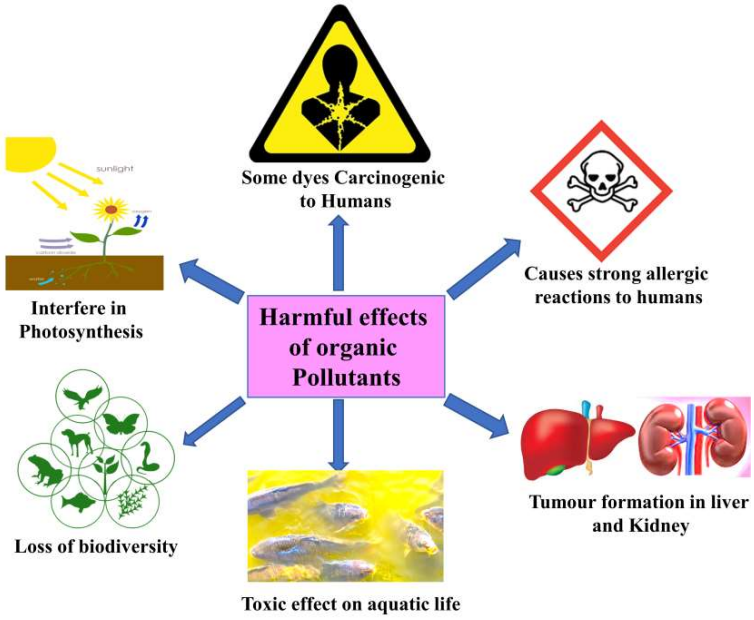

Fig. 1.2: Toxic effects of organic pollutants (El-Shahawi et al., 2010; Jones & De Voogt, et. al, 1999)

Organic pollutants include dyes, pesticides, herbicides, personal care products, solvents, etc.

1.1.1. Dyes

Dyes are organic substances with chromophores (conjugated -C=C-, -N=N-, and -CN) in their molecular structures. Functional groups such as NH_2, -OH, -COOH, $-SO_3H$ in these dyes are responsible for the increase in colour intensity and affinity to fibres (Oliveira et al., 2018). Textile, paper, plastic, leather, pottery, cosmetics, ink, food processing, and many more industries employ dyes. More than 1000,000 dyes are commercially available, with an annual production of over 7 lakh tons (Nipa et al., 2023). Most water-soluble dyes exhibit poor biodegradability and are sometimes difficult to detect at low concentrations. They are also toxic and recognized as carcinogenic and mutagenic. Using dye-contaminated can damage human organs such

as the kidney, liver, brain, etc., or cause skin allergies. Ten to twenty percent of all colours generated worldwide are discharged as textile effluents into the environment during dyeing (Adithya et al., 2021; Gianfreda et al., 2005; Pimentel et al., 2004).

A significant form of water pollution is the discharge of coloured wastewater into the environment. Oxidation, hydrolysis, or other chemical processes occurring during the wastewater processing can create more hazardous by-products. Thus, the degradation of dye effluents has drawn more and more attention. Among various dyes, this thesis focuses on the degradation of two dyes Rhodamine B (RhB) and Methyl orange (MO) (Fig. 1.3). RhB is a cationic dye produced by textiles industries, while MO is a common water-soluble azo dye extensively used in textile, paper, printing, and food industries (Cinelli et al., 2017; Farhan Hanafi & Sapawe, 2020).

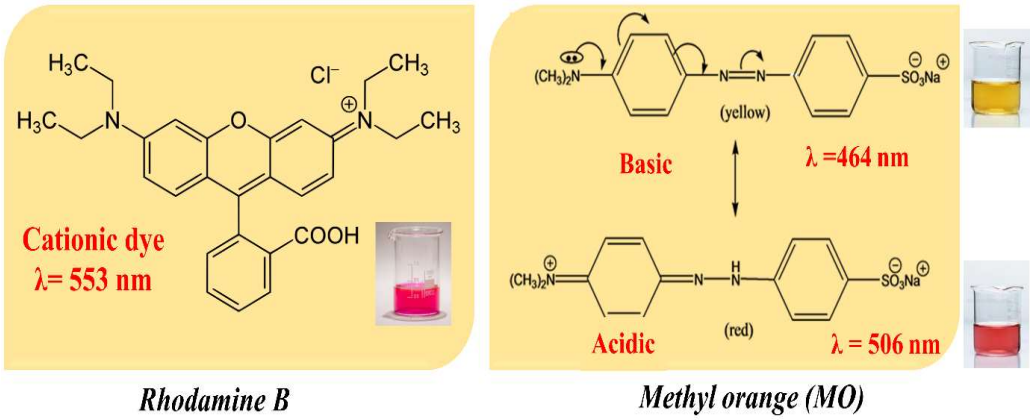

Fig. 1.3: The structures, colour, and absorption wavelength of RhB and MO dyes

1.1.2. Pharmaceutical pollutants

Another dangerous source of freshwater pollution is pharmaceutical pollution. Since therapeutic or pharmaceutical chemicals can quickly alter living things, their widespread use has drawn much attention. Additionally, pharmaceutical industries release many pharmaceutical by-products into the environment without following correct purification procedures. Anti-inflammatory and antibiotic drugs are extensively used to treat bacterial and fungal infections (Costa et al., 2019). Tetracycline (TET) and

Ciprofloxacin (CIP) are two globally popular pharmaceutical medication molecules (Fig. 1.4). TET and CIP molecules are stable to heat and light. Excessive use of these pharmaceutical compounds implies their partial metabolization in human or animal bodies. Partially metabolized antibiotics excreted by animals or humans can easily infiltrate water/environment through human waste or direct absorption into the environment. Such antibiotics in water increase the resistance of target bacterial colonies towards them (Daghrir & Drogui, 2013; Sharma et al., 2010).

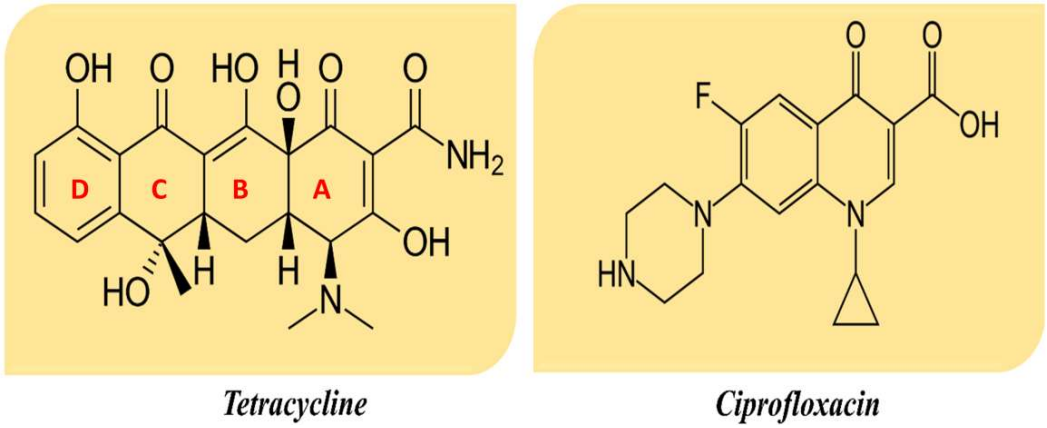

Fig. 1.4: Structures of TET and CIP

1.2. Removal or destruction of organic pollutants from wastewater

Before releasing wastewater into the aquatic environment, it is essential to decontaminate industrial effluents of harmful organic compounds effectively. Organic contaminant removal from water remains a problematic issue. The methods currently used for wastewater treatment can be roughly categorized into destructive and non-destructive approaches. Chemical and biological processes are destructive. Adsorption, filtration, flocculation, sedimentation, and membrane procedures are non-destructive separation methods (Gianfreda et al., 2005; Srivastav et al., 2018; Yang et al., 2005).

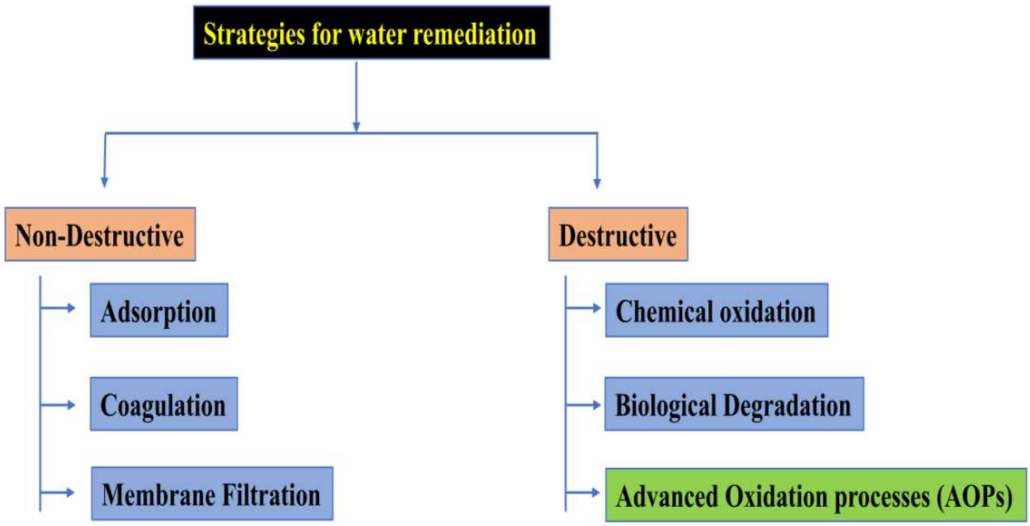

The primary disadvantage of non-destructive procedures is that they do not eliminate pollutants. Pollutant disposal is the main drawback of separation techniques. As an illustration, consider the disposal of pollutants in the sludge during coagulation processes; pollutants concentrated on adsorbent surfaces, and concentrated pollutant solutions due to membrane separation processes (Al-Tohamy et al., 2022).

Conversely, degradation processes transform polluting molecules into benign or environmental friendly by-products. These include advanced oxidation processes (AOP), biodegradation, and chemical oxidation methods. Scalability problems plague biological techniques. Chemical processes include precipitation, ion exchange, solvent extraction, chlorination, and oxidation-reduction reactions. These procedures are often unsuitable for efficient and cost-effective treatment of large volumes of water due to pH, pollutant concentration levels, solubility of the pollutant, etc. Chemical oxidation also includes photocatalysis. The latter does not involve any external agent for the oxidative degradation of organic pollutants (Al-Tohamy et al., 2022; Sathya et al., 2022).

AOPs are cost-effective and highly efficient oxidation techniques that are ideal for the extensive treatment of water pollutants. This family of procedures uses an external oxidant like H_2O_2 for generating reactive oxygen species (ROS) like hydroxyl

radicals (•OH) by reductive cleavage of the former. Other ROS like superoxide ($O_2^{\bullet-}$), hydroperoxyl (•OOH), and peroxy radicals (•OOR) may also be produced during this process. These may further aid the oxidative degradation of organic pollutants. Hydroxyl radicals have a high reduction potential (E_o = 2.8 V v/s SHE), making them the second most potent oxidant species (after fluorine), and they can oxidize almost all kinds of organic compounds. In many cases, these oxidants can completely mineralize organic contaminants. AOP processes often produce carbon dioxide, water, and a variety of inorganic ions (from heteroatom-containing organic pollutants). AOPs are the treatment methods of the twenty-first century because they may lower the concentration of pollutants from several hundred ppm to less than five ppb. Most AOPs involve the synthesis of •OH in a reaction system at temperatures and pressures close to ambient (Al-Tohamy et al., 2022; Andreozzi et al., 1999; Deng & Zhao, 2015; Sathya et al., 2022; Vilhunen & Sillanpää, 2010).

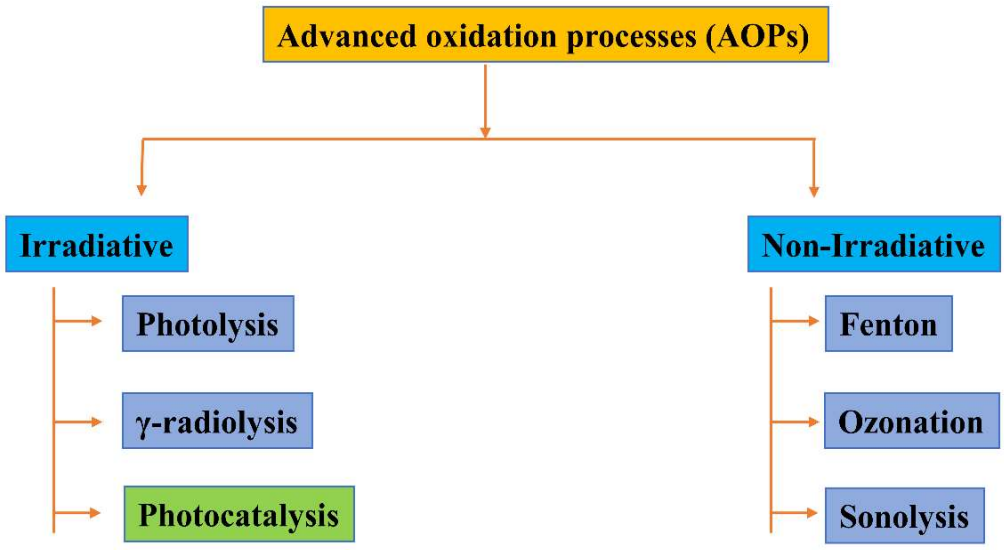

AOP's include O_3/UV, H_2O_2/UV, Fenton, O_3/UV, and photo-Fenton reactions. Ozonation procedures are not economical. The conventional or homogeneous Fenton process generates •OH free radicals by $Fe^{2+} + H_2O_2 \rightarrow Fe^{3+} + OH^- + OH\cdot$ reaction.

The process requires a constant supply of Fe^{2+} (Andreozzi et al., 1999; Sathya et al., 2022).

Conversely, photocatalysis only using light to power the oxidation of organic contaminants in water, without any external oxidant, is more cost-effective than the AOP class of techniques. Hence, this thesis focuses on designing and creating effective photocatalysts for treating water.

1.3. Photocatalysis

The word "photocatalysis" was first used in 1911 by German physicist Alexander Eibner (Baia et al., 2019). A photocatalyst is stimulated when UV or visible light is absorbed because the photon energy exceeds the material bandgap. The so-produced excited electron-hole pairs (or excitons) then interact with the appropriate substrate molecules to complete the electron transfer cycle. The photocatalyst returns to its initial state after the procedure is complete (Deng & Zhao, 2015). The use of photocatalysis in different applications, including the degradation of organic pollutants, the reduction of CO_2 and water splitting, the creation of H_2O_2, and others, offers significant promise (Jin, 2018). The advancement of photocatalysis is crucial because it opens the possibility of finding solutions to issues like environmental pollution and the depletion of fossil fuels (Wang et al., 2014).

1.4. Types of Photocatalysis

Photocatalysis is categorized into (i) homogeneous and (ii) heterogeneous classes

1.4.1. Homogeneous photocatalysis

The photocatalytic reaction is homogenous when the reactant and the catalyst are in the same phase making separation of homogeneous photocatalysts difficult. Hence, most homogeneous photocatalysts cannot be recycled or reused. Moreover, problems in separation imply that the photocatalyst can cause secondary pollution. Given this, the

construction of an appropriate class of heterogeneous photocatalysts is the focus of this thesis.

1.4.2. Heterogeneous photocatalysis

The photocatalyst and the reactants are distinct phases in heterogeneous photocatalysis. Heterogeneous photocatalysts exhibit advantages like a low secondary compound production rate, high recyclability, and efficiency. Semiconductor materials with a UV or visible range bandgap between valence (VB) and conduction band (CB) can act as heterogeneous photocatalysts (Osterloh, 2013). The discovery of TiO_2 as a photocatalyst for water splitting spurred the research on photocatalysis (Hu, 2012). Several researchers have employed TiO_2 as a photocatalyst for oxidizing organic contaminants from industrial wastewater discharges. Many semiconductor metal oxides have been employed as photocatalysts recently. These include Fe_2O_3 (Mishra & Chun, 2015), $Bi_2Ti_2O_7$ (Yao et al., 2004), ZnO (Look, 2001), SnO_2 (Xiong et al., 2018), WO_3 (Deb, 2008), Co_3O_4 (Feng & Zeng, 2003), CuO (Kannan et al., 2022), Cu_2O (Kerour et al., 2018), and NiO (Akbari et al., 2020). After WO_3, tungsten-based compounds like WS_2 (Cong et al., 2018), Bi_2WO_6 (L. Zhang et al., 2011), $MnWO_4$ (Joaquín-Morales et al., 2019), $FeWO_4$ (Rajagopal et al., 2010), $CoWO_4$ (Rajagopal et al., 2010), $NiWO_4$ (Ji et al., 2018), $CuWO_4$ (Yourey & Bartlett, 2011), $ZnWO_4$ (G. Huang et al., 2007), Ag_2WO_4 (Macedo et al., 2018), etc. These semiconductor photocatalysts have received attention because of their excellent physical and chemical characteristics, including their capacity for photon absorption, high stability, lack of toxicity, high activity, high surface area, and favourable electrical characteristics (Hu, 2012; Mishra & Chun, 2015; Osterloh, 2013; Yao et al., 2004)]. Fig. 1.5 displays the band edge positions and band gap energies of common semiconductor materials (Xu et al., 2018).

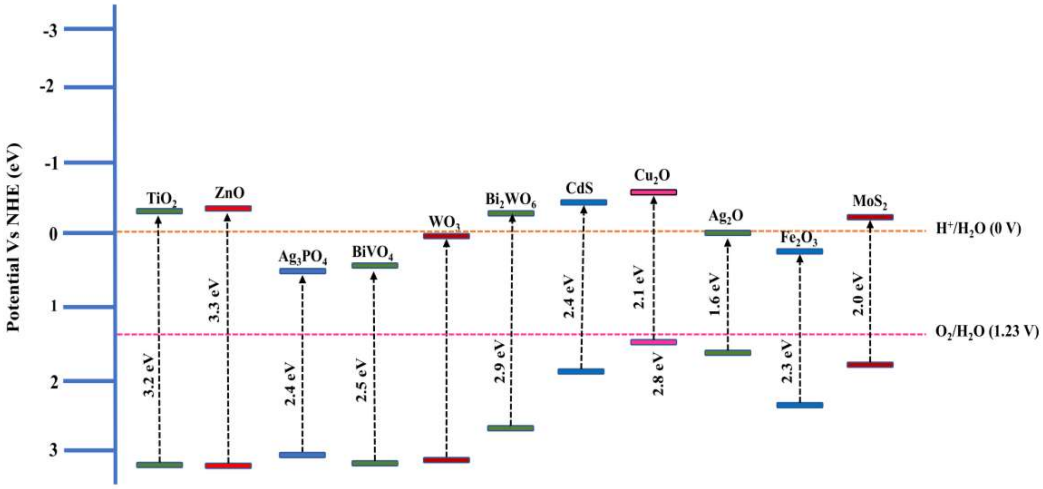

Fig. 1.5: Schematic representation of band edge position and band gap of common semiconductors

1.5. General Mechanism of Photocatalysis

CB (conduction band) refers to the lowest unoccupied energy band, and VB (valence band) is a semiconductor's highest occupied energy band. The band gap divides the VB and CB. Photo-excited electrons are stimulated from the semiconductor's VB to CB when a light source with photon energy (hv) strikes a semiconductor with lower band gap energy (Eg). Simultaneously, the process generates holes in the VB of the photocatalyst. The photogenerated electrons and holes have two options. They can reduce or oxidize species to drive possible photocatalytic reactions. Otherwise, the excited species can recombine radiatively or non-radiatively (heat generation). Recombination reduces the photocatalysis potential (photoexcited species) and must be minimized to enhance efficiency (Hu, 2012; Osterloh, 2013).

The photo-excited electrons and holes can generate reactive oxygen species depending on the VB and CB positions relative to the electrochemical series. The photocatalyst CB should be above (or more negative) the reduction potential of the species to be reduced. Superoxide radicals ($O_2^{\bullet -}$) form when the photoexcited electrons on the photocatalyst CB reduce dissolved oxygen. Holes can directly oxidize the target

organic molecule or hydroxide anions if the photocatalyst VB position is more positive. Water oxidation on photogenerated holes is also possible depending on the VB position (Mao et al., 2021).

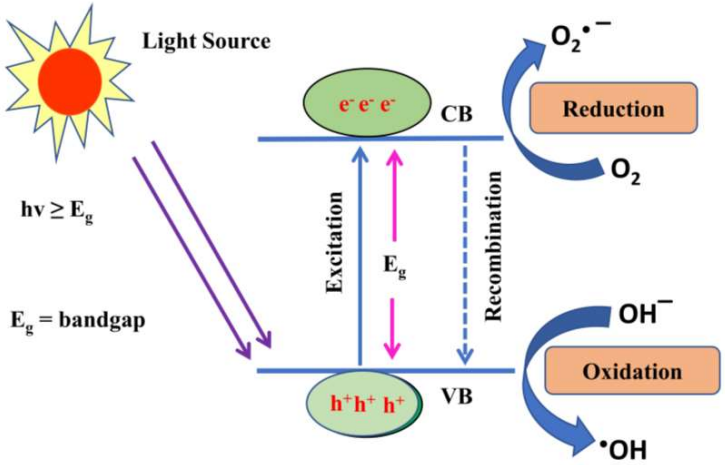

Fig. 1.6: Schematic describing the basic photocatalysis mechanism

Fig. 1.6 displays a schematic of typical processes in a photocatalytic system. Thus, to generate hydroxyl radicals through the oxidation of H_2O, the VB energy level must be higher than 2.8 V versus NHE. Similarly, to generate superoxide radicals by O_2 reduction, the CB should be more negative than -0.28 V versus NHE (Hu, 2012; L. Zhang et al., 2011).

1.6. Parameters for designing good photocatalyst

The semiconductor material should have a suitable band gap to absorb radiation and generate photo-excited species. The UV part of the solar electromagnetic spectrum is around ~5%, while ~45% is in the visible range (Ola & Maroto-Valer, 2015). Given this, investigators prefer photocatalysts that have a visible range bandgap. Photocatalysts photoexcited by visible light absorption make the maximum possible use of solar radiation. In other words, visible-range photocatalysts are energy efficient. Another issue is that the photoexcited electron-hole pair generation efficiency should be significantly higher than their recombination (Mao et al., 2021). In other words, the photoexcited species should have an increased life span. The latter ensures a high

fraction of the electrons and holes are available for possible reduction or oxidation reactions (Ola & Maroto-Valer, 2015). Furthermore, nanoparticles with higher surface area yield higher photocatalytic efficiencies than their bulk counterparts due to improved reactant adsorption properties (Fig. 1.7). Specific adsorption properties of the reactants to the photocatalyst components can enhance the possible oxidation or reduction reaction kinetics (Singh et al., 2020).

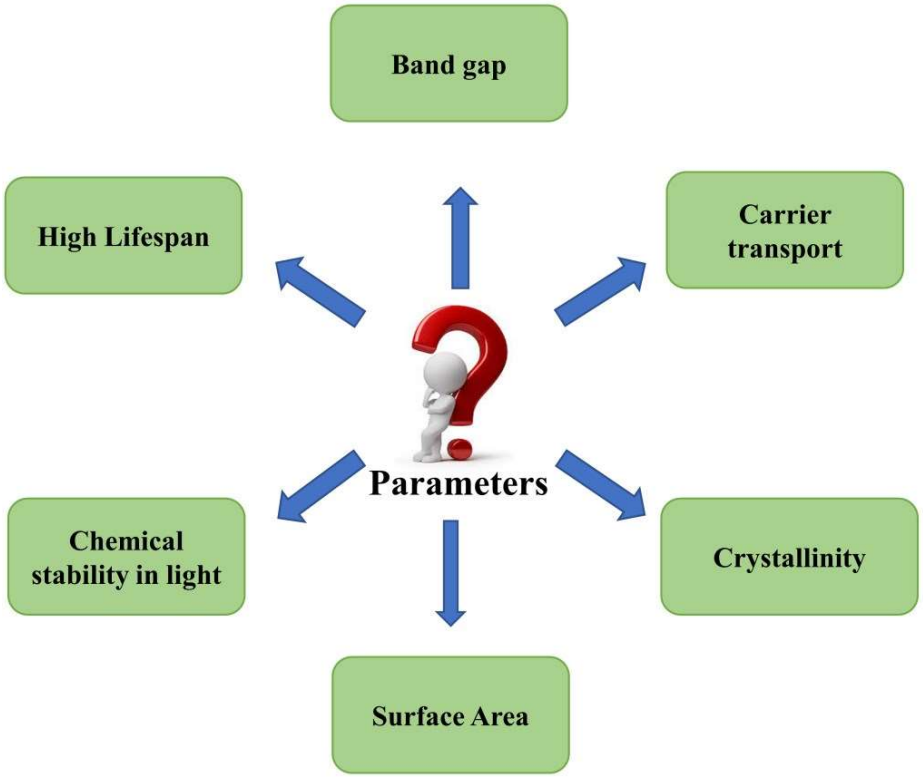

Fig. 1.7: Parameters to be considered for efficient photocatalyst design

1.7. Challenges in designing promising photocatalysts

Photocatalysis consists of four stages. These are (i) light absorption; (ii) charge separation; (iii) charge migration (with potential recombination); and (iv) charge consumption for redox reactions. The last stage depends on the VB and CB positions of the photocatalyst (Das et al., 2022; Singh et al., 2020). This stage also requires the adsorption of the reactants on the photocatalyst surface. Though adsorption is necessary, excessively strong adsorption of one of the reactants can poison the catalyst

surface. The latter implies that only one reactant adsorbs, and the adsorption of the other reactant is negligible. A photocatalytic reaction can proceed efficiently only when the reduction and oxidation occur simultaneously. Alternatively, very poor adsorption could impair the reaction's kinetics. As a result, the reactants' adsorption strength should be just right—neither too weak nor too strong. The implanting photocatalyst nanoparticles on a support material with favourable adsorption properties for the involved reactants is a crucial method to get around this issue (Augugliaro et al., 2006). The reaction's kinetics are accelerated by supports with excellent adsorption properties, even though the main photocatalyst may weakly adsorb the desired reactant molecule (Fig. 1.8).

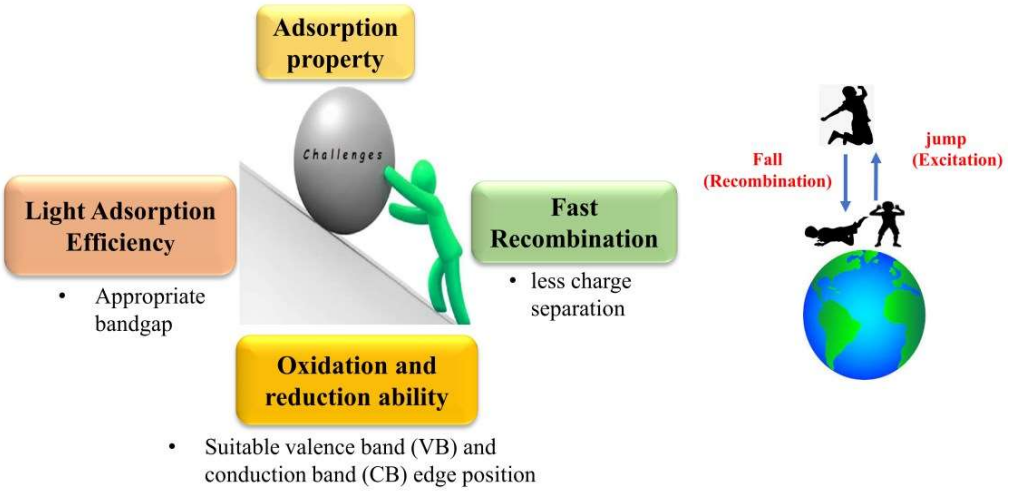

Fig. 1.8: Challenges in designing efficient photocatalysts

A photocatalyst can use its CB electrons to reduce oxygen to superoxide radicals or hydrogen peroxide. These reactive species then attack and reduce the target molecules. In parallel, holes move to the semiconductor material's surface, where they oxidize donor species. This method avoids the requirement for direct contact between the reactant molecules that need to be reduced and oxidized. The adsorbed species' redox potentials and the photocatalyst's CB and VB positions determine how charges are transferred between them and the semiconductor. The molecule that will be oxidized

should have a lower redox potential than the VB. Like this, the electron recipient's (or the molecule to be reduced's) reduction potential should be higher than the CB (Xiong & Tang, 2021). The competing processes' relative speed determines whether recombination occurs or photo-excited species (holes and electrons) can react with the adsorbed reactants (Fig. 1.9).

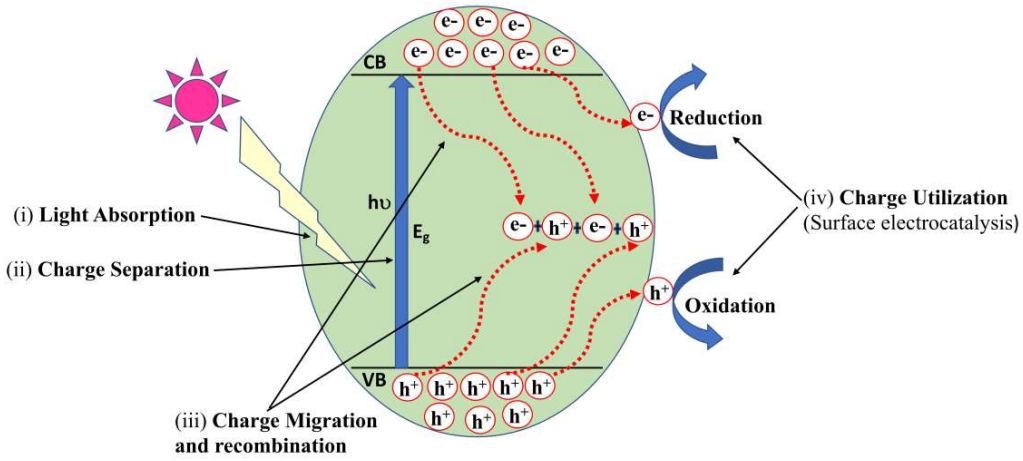

Fig. 1.9: Schematic representation of various phenomena possible after photo-excitation (Xiong & Tang, 2021)

Recombination may occur on the surface or in the bulk of the photocatalyst particles (Fig. 1.9). Additionally, the energy emitted during the recombination of holes and electrons may be radiative or non-radiative. Therefore, recombination is a crucial process that governs the excitons' lifetime. The lifespan of the charged species increases dramatically if the charges are separated, which improves the likelihood that the electrons or holes will react with the reactants adsorbed on the surface of the photocatalyst. The ultimate goal is to increase the amount of photo-excited holes and electrons that can reach the photocatalyst's surface without recombining. In that circumstance, there is a significant increase in the likelihood that the excited species will react with the target reactant molecules (Padmanabhan et al., 2021).

1.8. Fundamental Strategies to overcome challenges associated with Photocatalysts

Strong charge-carrier mobility, minimal recombination energy losses, and appropriate band edge placements are necessary for semiconductor materials employed as photocatalysts. Recombination, charge separation, and charge migration in photocatalysts are all impacted by many circumstances. The photocatalyst's crystallinity is one of the factors. The rates of recombination are substantially lower in more crystalline semiconductors. Increasing crystallinity by annealing is a common method for improving photocatalytic performance. However, the method has its drawbacks due to the loss of surface-active sites (Kanakaraju & Chandrasekaran, 2023). A co-catalyst can be used with the principal photocatalyst to control charge separation and migration. For instance, metal-semiconductor heterostructures have enhanced photocatalytic capabilities. Improved charge separation might also result from fabricating a composite of two semiconductors. Charge separation can also be improved by affixing photoactive organic molecules to the semiconductor surface. Another method widely employed to postpone recombination and promote charge separation is the appropriate doping of semiconductors (H. Zhao et al., 2022).

1.8.1. Defects and doping

Another method for enhancing or changing a single-phase semiconductor's photocatalytic capabilities is doping with a metal or non-metal ion. Doping in semiconductors involves purposefully introducing foreign substances into the host lattice structure. Whether a metal or a non-metal is the inserted foreign element, doping may be cationic or anionic. The foreign element can replace an atom in the host lattice structure or occupy an interstitial location (void space). Doping can alter the electronic structure and adsorption characteristics of a semiconductor (Samadi et al., 2016). A schematic illustrating the impact of doping in photocatalysis can be seen in Fig. 1.10.

According to Wu et al., 2010 and T. Zhang et al., 2006 co-workers, semiconductor crystals come in various forms and facets that display discrete charge separation in particular orientations. It has been discovered that many surface defects exhibit distinctive trapping of electrons or holes that cause charge separation. The latter stops photogenerated electrons and holes from recombining quickly (Hu, 2012; Osterloh, 2013). For instance, researchers have found that doping TiO_2 with 0.5–1% of metal ions such as Fe^{3+}, Mo^{5+}, and Ru^{3+} increases photocatalytic effectiveness (Choi et al., 1994). Oxygen vacancies acting as active sites for photochemical processes or as sites anchoring co-catalysts can increase photocatalytic activity. Doping can also alter the semiconductor's band structure by adding new bands or dopant levels (S. Zhang et al., 2020). The bandgap may become narrower or wider depending on where these band levels are located (Fig 1.10).

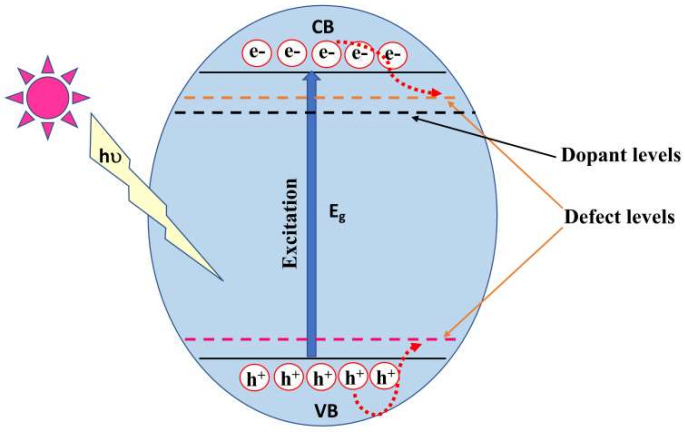

Fig. 1.10: Effect of doping on the band position of semiconductors

1.8.2. Heterostructure formation

Heterostructure photocatalysts are composites made of two or more semiconductors. Linking two separate semiconductors with acceptable VB and CB positions can achieve better charge separation and distinctive adsorption capabilities. In the literature, there have been reports on synthesizing composite photocatalysts such as TiO_2/CuS (S. Huang et al., 2022), $MoS_2/Fe_3O_4/Cu_2O$ (W. Li et al., 2021), NiO/TiO_2 (Shifu et al.,

2008), etc. The two components' VB and CB positions must also be staggered for greater charge separation. One can construct two different forms of photocatalyst heterostructures with such uneven band alignments. These are composite photocatalysts based on the Z-scheme and p-n heterojunction (Type II). These two different composite photocatalyst types' electron transport mechanisms are shown in Fig. 1.11 (J. Li et al., 2022).

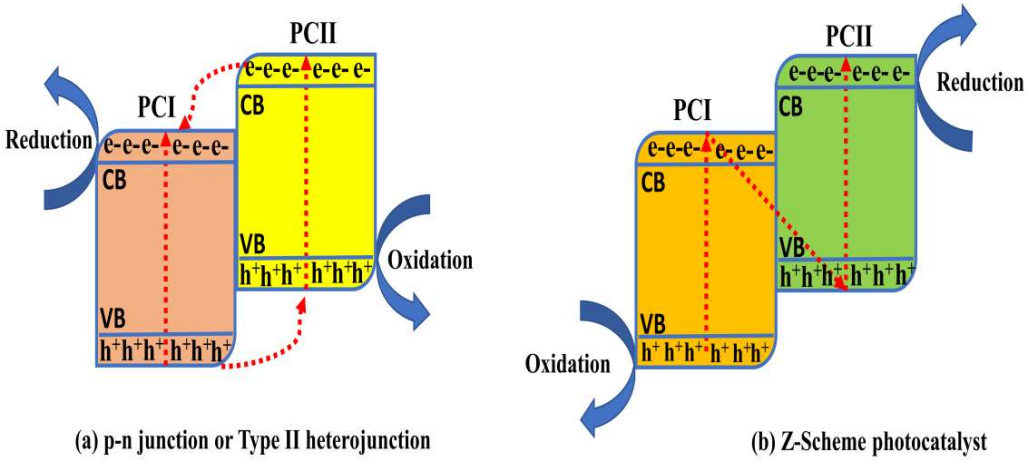

Fig 1.11: Schematic of electron transport mechanisms in (a) p-n Junction (Type-II) and (b) Z-scheme photocatalyst

1.8.2.1. p-n heterojunction/Type II heterojunction

There are p-type and n-type semiconductor components in a typical p-n heterojunction. A p-n interface forms due to the migration of extra electrons from the n-type semiconductor side and holes from the p-type portion. As a result, until the equilibrium of the Fermi level is reached, the electrons tend to spread from n-type to p-type (Peng et al., 2014). At the heterojunction photocatalyst contact, an internal electric field is subsequently generated. The emission of electron-hole pairs from such photocatalysts occurs when light with an energy higher than the bandgaps of the individual semiconductors is used. The more negatively charged photoexcited electrons on the p-type CB migrate to the n-type CB, which is comparatively positively charged (Fig 1.11a). Likewise, holes shift from the VB with a higher positive value (n-type) to one

with a lower positive value (p-type). As a result, the charge carriers are separated by an accumulation of electrons on the component with a less negative CB and holes on the component with a more positive VB position (Z. Zhang et al., 2010). AgI/$BiVO_4$ (W. Zhao et al., 2019), NiS/CdS (Fan et al., 2022), ZnO/ZnSe (Cho et al., 2011) and others are described p-n junction (type II) heterostructures.

1.8.2.1. Z-scheme Photocatalyst

Despite the excellent charge separation that the p-n heterojunction demonstrates, the reaction driving forces are modest due to the lower oxidation and reduction potentials of the electron-rich VB and hole-rich CB. This issue can be resolved with a Z-scheme photocatalyst. An amalgam of two or more n-type or two or more p-type semiconductors (either n-type or p-type) with staggered band alignments makes up a typical Z-scheme photocatalyst. Photo-excitation generates electrons and holes in both components of the composite. The photo-excited electrons on the CB of one semiconductor quench the VB holes of the second component, as shown in Fig. 1.11b. Electrons collect on the more negative CB of the other semiconductor and holes on the more positive VB of the first semiconductor. The oxidation and reduction potential of the hole-rich VB and the electron-rich CB enhance the photocatalyst's redox capacity (Xu et al., 2018). Therefore, a Z-scheme mechanism enhances charge separation and the photocatalyst's redox capability. For instance, WO_3/Bi_2WO_6 (Jia et al., 2023), Fe_2O_3/g-C_3N_4 (Liu et al., 2023), In_2S_3/Bi_2WO_6 (He et al., 2022), $BiVO_4$/CdS (Xia et al., 2023), etc. are reported as Z-scheme photocatalyst.

1.9. Literature Review and Research Gap

In 1972 Fushishima and Honda demonstrated TiO_2 as a photoanode in the photoelectrochemical water splitting (Fujishima A & Honda K., 1972). Subsequently, the photocatalytic research interest has been devoted to semiconductor photocatalysis. It has a wide band gap of 3.2eV, which limits its application to UV radiation only

(Etacheri et al., 2015). Compared with TiO_2 photocatalyst, WO_3 has a bandgap in the 2.7-2.8 eV range. (Butler et al., 1976) published the first report on the photocatalytic properties of WO_3. However, the lower CB position of WO_3 (0.5V vs. NHE) and fast recombination of charge carriers retards its redox ability. The limitations in the photocatalytic properties of WO_3 can be reduced by its composition or by fabricating its composites. WO_3 composition change can be brought about by doping (Loka & Lee, 2022). Joining the WO_3 nanostructure with another inorganic or organic semiconductor component gives its composites or heterojunctions. Another method is precipitating noble metal (co-catalyst) nanostructures on WO_3 nanoparticles. Modifications in morphology, particle size, and surface defects can also increase the lifetime of the photogenerated charge carriers (S. G. Kumar & Rao, 2017).

Along with WO_3, much photocatalysis research has also been conducted on other tungsten-based semiconductor materials. These include WS_2 (Cong et al., 2018), Bi_2WO_6 (C. Huang et al., 2019), $MnWO_4$ (Zinatloo-Ajabshir et al., 2021), $FeWO_4$ (Gao & Liu, 2017), $CuWO_4$ (Raizada et al., 2020), etc. All these semiconductors have demonstrated great potential for organic pollutant remediation. Kudo and Hijii first synthesized Bi_2WO_6 in 1999 and utilized it as an oxygen evolution catalyst (Kudo A & Hijii S, 1999). In 2008, Zhou et al. 2009 reported RhB degradation by hierarchical $FeWO_4$ photocatalyst nanostructures. Bera et al., 2014 reported CdS/$FeWO_4$ heterojunctions with increased charge carrier lifetime and photocatalytic activity. Researchers also explored $CuWO_4$ as a photoanode in photoelectrochemical water splitting (Yourey & Bartlett, 2011).

This thesis introduces $CuWO_4$-based heterostructures for visible-light-driven photocatalytic degradation of organic pollutants. The thesis also discusses the hierarchical structure and exposed facets that boost the photocatalytic activity.

1.9.1. $CuWO_4$

Benko's research group published the first photoelectrochemical water-splitting study using $CuWO_4$ photocatalyst in 1982 (Benko et al., 1982). $CuWO_4$ is an n-type semiconductor with a 2.2-2.4 eV bandgap, moderate toxicity, and exceptional stability against photo-corrosion and chemical corrosion in a neutral and acidic medium. It is a possible photocatalyst for water splitting. There have been attempts to increase this photocatalyst's photocatalytic and photoelectrochemical performance (Raizada et al., 2020).

$CuWO_4$ typically has a wolframite-type crystal structure. The $CuWO_4$ triclinic form crystallizes with unit cell parameters a = 4.7026 A°, b = 5.8389 A°, c = 4.8784 A°, α= 91.677°, β= 92.469°, γ= 82.805° (Tian et al., 2019) (Fig. 1.12). There are four non-equivalent oxygen atom positions. Cations occupy half the octahedral sites in the hexagonal close-packing (hcp) oxygen anion sub-lattice. Six oxygen atoms bond to each metal atom. $CuWO_4$'s valence band has O2p and Cu3d orbitals. $CuWO_4$ has a higher VB than WO_3 due to the mixing of the 2p and 3d atomic orbitals of O and Cu, respectively. The bandgap is reduced, making possible the utilization of a larger region of the visible-light spectrum. $CuWO_4$'s CB is comprised of 5d and 3d orbitals of W and Cu, respectively (Raizada et al., 2020).

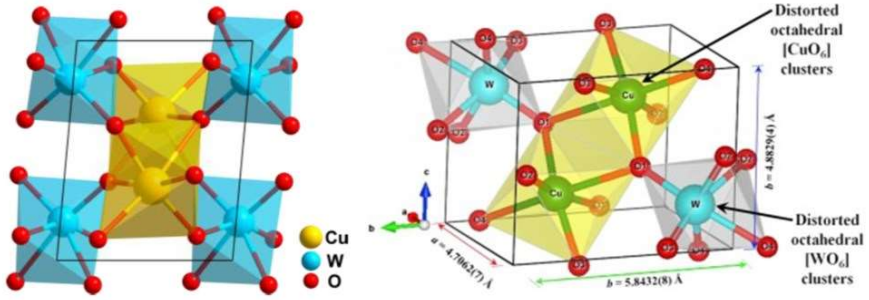

Fig. 1.12: Crystal structure of $CuWO_4$ (Tian et al., 2019)

Although $CuWO_4$ has many applications, it does have significant restrictions that reduce its photocatalytic efficacy. Low photocurrent (10.7mA/cm^2) and electron-

hole pair (EHP) recombination need addressing to achieve improved photocatalytic performance. Several techniques for inhibiting EHP recombination have been explored, including coupling $CuWO_4$ with electron scavengers such as metallic and non-metallic dopants, co-catalysts, semiconductors, etc. Semiconductor heterostructures with $CuWO_4$ as one of the components have improved photocatalytic activity. For example, $BiFeO_3/CuWO_4$ (Ramezanalizadeh & Manteghi, 2017), $VO_2/CuWO_4$ (Dashtian et al., 2018), $CuWO_4$/ZnO (Chen et al., 2020), $CuWO_4$/MWCNT(Gaillard et al., 2013), g-$C_3N_4/Fe_3O_4/CuWO_4$ (Habibi-Yangjeh & Mousavi, 2018), g-$C_3N_4/CuWO_4$ (Vinesh et al., 2022), $CuWO_4/Bi_2S_3$ (Askari et al., 2020) and others have exhibited excellent photocatalytic activity towards certain organic compounds. However, the literature of this research area has not reported Ag-based semiconductor/$CuWO_4$ nanocomposites.

1.9.2. Ag-based semiconductors

Ag-based semiconductors are of interest owing to their better conductivity and lower band gap. They include Ag/Ag_2O (K. Li et al., 2022), Ag_2S (Yu et al., 2019), AgX (Cl, Br, I) (Mao et al., 2018), Ag_3PO_4 (L. Luo et al., 2014), Ag_3VO_4 (Raizada et al., 2019), Ag_2CO_3 (Dai et al., 2012), Ag_2MoO_4 (Sousa et al., 2020) and others. Generally, their band gap energy is less than 3.0 eV. Thus, all Ag-based semiconductors are susceptible to visible light irradiation. AgCl, Ag_2O, and Ag_2S have much lower band gap energies (~2.0 eV). Because of their high visible light absorption, significant efforts have been put into designing, preparing, and characterizing Ag-based photocatalysts. Fig. 1.13 shows utilized Ag-based semiconductors' band gap energies, CB, and VB positions.

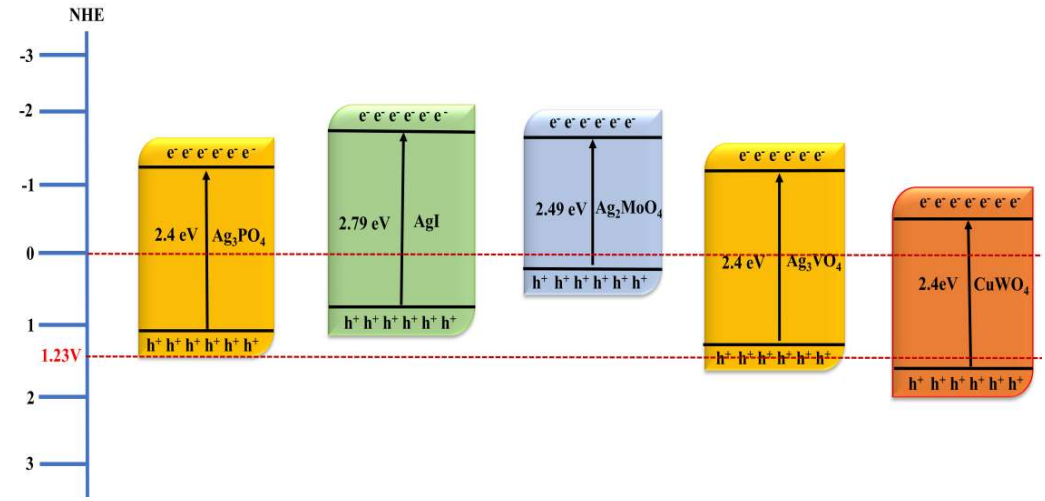

Fig. 1.13: Some Ag-based semiconductors' band gap energies, VB, and CB positions relative to $CuWO_4$ values

1.9.3. Literature Review on Z-Scheme Photocatalysts

Recently, the focus has been on creating unique and more effective Z-scheme composites. Thus, many Z-scheme nanocomposites have been investigated through the synthesis of heterojunction composites such as g-C_3N_4/Ag/MoS_2 (Lu et al., 2017), g-C_3N_4/$CuWO_4$ (S. Zhou et al., 2021), g-C_3N_4/Ag_2WO_4 (Zhu et al., 2017), TiO_2/CdS (Meng et al., 2017), CdS/Co_9S_8 (Qiu et al., 2017), Ag/AgBr/g-C_3N_4 (Yan et al., 2020), Ag_3PO_4/g-C_3N_4 (L. Zhou et al., 2017), $BiVO_4$/g-C_3N_4 (J. Zhao et al., 2016). There are now two popular varieties of solid-state Z-scheme photocatalysts. One uses a direct Z-scheme technique, while the other uses an indirect one. Direct Z-scheme photocatalysts are photocatalysts that only have two semiconductor components (Fig. 1.14). A conducting metal nanostructure connects the semiconductor components in an indirect Z-scheme photocatalyst. For instance, the 'Ag' component connects the g-C_3N_4 and MoS_2 semiconductors in the composite g-C_3N_4/Ag/MoS_2 photocatalyst. Direct Z-scheme photocatalysts are efficient in spatially separating photogenerated electron-hole pairs. They also improve the reduction and oxidation capabilities of the photocatalytic

system. Some direct Z-scheme photocatalysts are $BaFe_2O_4$/BiOCl (Tan et al., 2023), $ZnFe_2O_4$/$CuWO_4$ (J. Luo et al., 2022), Ag_3PO_4/Bi_2WO_6 (Ma et al., 2018), etc.

$CuWO_4$ based Z-scheme photocatalysts reported in literature are $CuWO_4$/Bi_2S_3 (Askari et al., 2020), VO_2/$CuWO_4$ (Dashtian et al., 2018), $ZnFe_2O_4$/$CuWO_4$ (J. Luo et al., 2022), $CuWO_4$/BiOCl (Chang et al., 2022), etc. There are several reports available on Z-scheme photocatalysts with a Ag-based semiconductor as one of the components. Some examples are Ag_2CO_3/Ag/WO_3 (X. Yuan et al., 2017), Ag_3PO_4/Bi_2WO_6 (Ma et al., 2018), SnS_2/Ag_3VO_4 (Q. Li et al., 2023), etc. However, except the reports in this thesis, there are very few publications on Ag-based semiconductor/$CuWO_4$ Z-scheme photocatalysts.

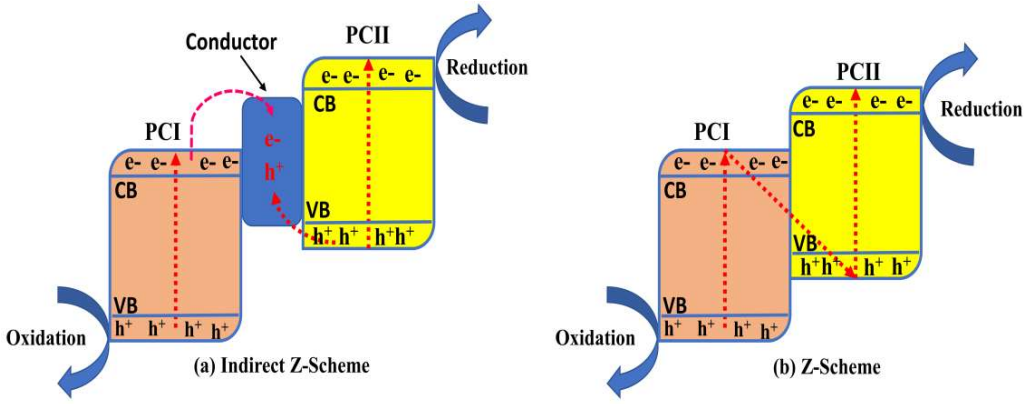

Fig. 1.14: Schematic representation of indirect and direct Z-scheme photocatalyst

As shown in Fig 1.13, Ag-based semiconductors and $CuWO_4$ have suitable band edge positions and fulfill other requirements for fabricating Z-scheme photocatalysts. This thesis will investigate various Ag-based semiconductor/$CuWO_4$ nanocomposites *viz.* AgI/$CuWO_4$, Ag_3PO_4/$CuWO_4$, Ag_3VO_4/$CuWO_4$, Ag_2MoO_4/$CuWO_4$ Z-scheme photocatalysts for photocatalytic degradation of organic contaminants.

1.10. Fabrication Strategies for Z-scheme Photocatalyst

Numerous considerations must be made regarding the design and synthesis of direct Z-scheme photocatalysts. The two semiconductor components with staggered band structures must satisfy the criterion that one component has higher CB and VB locations

and a smaller work function (higher Fermi level) than the other. Figure 4a illustrates this requirement for the successful preparation of direct Z-scheme photocatalysts. Considerations should be made for morphology, exposed facets, surface states, and interfacial qualities. When two components are put together, they may show a variety of geometric configurations, which could impact how well they work. Various methods have been adopted for the synthesis of Z-scheme photocatalysts. Some of them are discussed below (C. Li et al., 2023; X. Li et al., 2021).

1.10.1. Deposition–precipitation method

Direct Z-scheme heterojunctions are synthesized using the efficient and flexible method of deposition-precipitation. The process is usually carried out by depositing one component at a low temperature on the surface of another component. The first component is used as a substrate to provide enough surface sites for in-situ nucleation and growth of another component. The procedure ensures contact between the two phases but suppresses the aggregation of nanostructures of the deposited component. Such deposition protocol facilitates charge carrier separation and transfer between these two components. A subsequent post-calcination process increases the material's crystallinity. The latter reduces charge carrier recombination and improves photocatalytic performance. For instance, a directed diffusion and charge-induced deposition method at room temperature successfully decorated the surface of MoO_3 nanobelts with AgBr quantum dots (X. Li et al., 2021).

1.10.2. Hydrothermal and solvothermal method

High temperature and pressure are used in a sealed autoclave during a typical hydrothermal procedure to create semiconductor nanoparticles with high crystallinity and a limited size distribution. This technique enables the direct synthesis of Z-scheme photocatalysts without any post-treatment. For instance, the Bi_2WO_6/g-C_3N_4 composite was prepared using a hydrothermal technique (Y. Zhao et al., 2018).

1.10.3. Solid-state synthesis

A typical calcination technique is carried out at high temperatures in an air- or inert-gas-filled muffle or tube furnace. The produced samples' morphology, crystallinity, interfacial characteristics, and phase structures are greatly influenced by the heating rate, calcination temperature, and duration. A good example is the creation of a novel Fe_2O_3/g-C_3N_4 composite that resembles nanorods (Xiao D et al., 2015).

1.10.4. Ion exchange method

The parent ionic crystal is exposed to new ions during the ion exchange process, which replaces ions in the crystal while leaving the framework unaltered. Because of the increased surface access and lower activation barrier to the diffusing ions than the bulk material, ion exchange on nanocrystals can occur quickly at high temperatures. It's important to note that ion exchange provides a flexible method for creating atomically precise, high-quality interfacial contact between the two semiconductors. For example, the roxbyite Cu_7S_4 nanocrystal was chosen as the starting template to create the c-MnS/Cu_7S_4 Janus-like structure by switching the Cu^{2+} ions for Mn^{2+} ions (Q. Yuan et al., 2017).

1.10.5. Electrospinning method

In recent years, electrospinning has developed into a flexible synthesis method to create materials that resemble fibers. For this technique, a syringe with a metallic needle, a collector, and direct current power is often required. The electrospinning apparatus is straightforward, making the process inexpensive and scalable. Notably, the crystallinity of the resultant materials must always be improved by a post-heating process. For instance, foam-assisted electrospinning followed by solution-dipping fabricated mesoporous TiO_2/WO_3/g-C_3N_4 ternary hybrid nanofibers (Ibrahim & Gondal, 2021).

1.10.6. Self-assembly method

Self-assembly is the process by which isolated parts spontaneously arrange themselves into a structured arrangement to reduce the total system's free energy. For instance, the surface of ZnO nanoplates was spontaneously covered with g-C_3N_4 sheets to reduce the surface energy, leading to a core-shell N-doped ZnO/g-C_3N_4 composite. The composite had enhanced carrier transfer efficiency (S. Kumar et al., 2014).

1.11. Objective of this thesis

According to the extensive literature review in the preceding sections, several studies have been conducted on $CuWO_4$-based heterojunctions. The usage of $CuWO_4$ phases in the fabrication of Z-scheme photocatalysts using Ag-based photocatalysts is virtually unexplored. As a result, this thesis focuses on synthesizing Z-scheme photocatalysts such as AgI/$CuWO_4$, Ag_3PO_4/$CuWO_4$, Ag_3VO_4/$CuWO_4$, and Ag_2MoO_4/$CuWO_4$. X-ray diffraction (XRD), Transmission electron microscopy (TEM), and X-ray photoelectron spectroscopy (XPS) were used to characterize these heterostructures. Bandgap was determined using solid-state UV-visible diffuse reflectance spectroscopy.

These photocatalysts have been investigated for their photocatalytic activity towards visible light degradation of ciprofloxacin (CIP), tetracycline (TET), Rhodamine (RhB), and methyl orange (MO) in their aqueous solutions. Further, a systematic approach has been adopted to explore the mechanism and kinetics of photocatalytic degradation (Fig. 1.15). The thesis's point-by-point aims are listed below.

- AgI/$CuWO_4$ Z-scheme photocatalyst for the degradation of organic pollutants: Experimental studies.
- Experimental investigations on Z-scheme visible light Ag_3PO_4/$CuWO_4$ photocatalysts for antibiotic degradation.
- Investigations on Z-scheme Ag_3VO_4/$CuWO_4$ for organic pollutant degradation.

- $Ag_2MoO_4/CuWO_4$ Z-scheme photocatalysts for the degradation of organic pollutants.

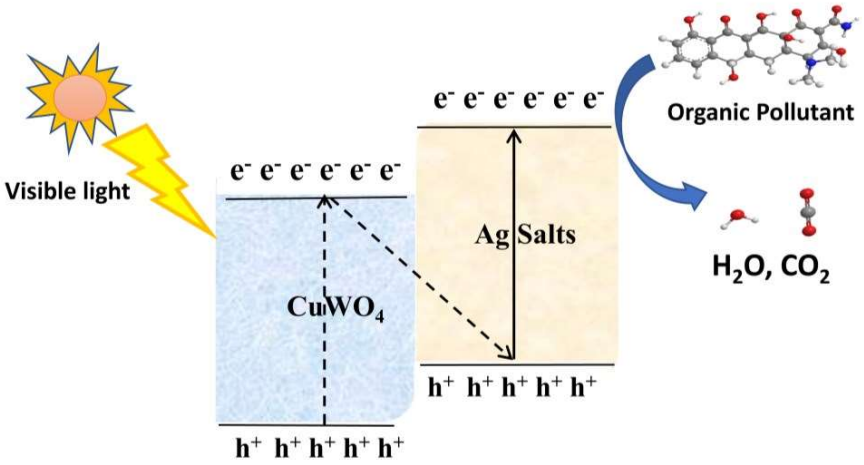

Fig. 1.15: Schematic representation of the objective of this thesis for the fabrication of Ag-based semiconductor/$CuWO_4$ nanocomposites for organic pollutant degradation